Published in final edited form as:
Calcif Tissue Int. 2011 September ; 89(3): 179–191. doi:10.1007/s00223-011-9505-1.

VDR Haploinsufficiency Impacts Body Composition and Skeletal Acquisition in a Gender-Specific Manner

Francisco J. A. de Paula,
Maine Medical Center Research Institute, Research Drive 81, Scarborough, ME 04074-7205, USA; Department of Internal Medicine, School of Medicine of Ribeirão Preto, USP, Av. Bandeirantes 3900, Ribeirão Preto, SP 14049-900, Brazil fjpaula@fmrp.usp.br

Ingrid Dick-de-Paula,
Maine Medical Center Research Institute, Research Drive 81, Scarborough, ME 04074-7205, USA; Department of Internal Medicine, School of Medicine of Ribeirão Preto, USP, Av. Bandeirantes 3900, Ribeirão Preto, SP 14049-900, Brazil idickp@gmail.com

Sheila Bornstein,
Maine Medical Center Research Institute, Research Drive 81, Scarborough, ME 04074-7205, USA bornss@mmc.org

Bahman Rostama,
Maine Medical Center Research Institute, Research Drive 81, Scarborough, ME 04074-7205, USA bahman.rostama@maine.edu

Phuong Le,
Maine Medical Center Research Institute, Research Drive 81, Scarborough, ME 04074-7205, USA lep@mmc.org

Sutada Lotinun,
Department of Oral Medicine, Infection and Immunity, Harvard School of Dental Medicine, Boston, MA 02115, USA Sutada_Lotinun@hsdm.harvard.edu

Roland Baron, and
Harvard Medical School and School of Dental Medicine, and Endocrine Unit, Massachusetts General Hospital, Boston, MA, USA roland_baron@hms.harvard.edu

Clifford J. Rosen
Maine Medical Center Research Institute, Research Drive 81, Scarborough, ME 04074-7205, USA

Abstract

The vitamin D receptor (VDR) is crucial for virtually all of vitamin D's actions and is thought to be ubiquitously expressed. We hypothesized that disruption of one allele of the VDR gene would impact bone development and would have metabolic consequences. Body composition and bone mass (BMD) in VDR heterozygous (VDR HET) mice were compared to those obtained in male and female VDR KO and WT mice at 8 weeks of age. Male mice were also evaluated at 16 weeks, and bone marrow mesenchymal stem cell (MSC) differentiation was evaluated in VDR female mice. Additionally, female VDR HET and WT mice received intermittent PTH treatment or vehicle (VH) for 4 weeks. BMD was determined at baseline and after treatment. MRI was done in

C. J. Rosen rosenc@mmc.org.

The authors have stated that they have no conflict of interest.

vivo at the end of treatment; μCT and bone histomorphometry were performed after killing the animals. VDR HET male mice had normal skeletal development until 16 weeks of age but showed significantly less gain in fat mass than WT mice. In contrast, female VDR HET mice showed decreased total-body BMD at age 8 weeks but ad a normal skeletal response to PTH. MSC differentiation was also impaired in VDR HET female mice. Thus, female VDR HET mice show early impairment in bone acquisition, while male VDR HET mice exhibit a lean phenotype. Our results indicate that the VDR HET mouse is a useful model for studying the metabolic and skeletal impact of decreased vitamin D sensitivity.

Keywords

Vitamin D; Parathyroid hormone; Body composition

The secosteroid vitamin D acts through a nuclear receptor (vitamin D receptor [VDR]) to modulate the transcription of multiple target genes in many tissues. Unique in the context of vitamins or hormones, vitamin D can be derived from exogenous dietary sources or can be endogenously synthesized from 7-dehydrocholesterol by a nonenzymatic ultraviolet B (290–315 nm)–mediated reaction [1, 2]. Subsequently, vitamin D activation requires two hydroxylations, the first occurring in the liver to form 25-hydroxyvitamin D (25[OH]D). This intermediary molecule has been largely used as a surrogate indicator for the assessment of vitamin D exposure [3]. The second, a renal hydroxylation, is responsible for the final synthesis of the systemically active metabolite $1,25(OH)_2D$, which is tightly controlled by parathyroid hormone (PTH), serum phosphate, and FGF-23. PTH serum levels are inversely associated with 25(OH)D concentrations and have been used in conjunction with serum vitamin D levels to diagnosis vitamin D deficiency [4, 5].

Vitamin D has a pivotal role in the maintenance of calcium and phosphorus homeostasis by direct actions on the intestine, bone, and parathyroid gland. Severe vitamin D deficiency is associated with impaired mineralization, proximal muscle weakness, bone pain, and osteomalacia. Recently, the contribution of vitamin D to bone mineralization has been reassessed in light of the finding that the skeletal phenotype of VDR knockout (KO) mice can be restored by maintenance on a high-calcium rescue diet [6,7]. In parallel, the use of genetically engineered mice (absence of VDR or 25-OHD-1α-hydroxylase [CYP27B1]) has helped investigators recognize the physiologic versatility of vitamin D [8]. VDR expression has been identified in almost all human tissues. Also, the spectrum of non-classical vitamin D actions has grown to include immunomodulation, cardiovascular regulation through blood pressure control and direct myocardial actions, control of energy expenditure, muscle function, and inhibition of cell proliferation in several tissues [8–10].

Recently, it has been suggested that different tissues have distinct thresholds to manifest vitamin D deficiency alterations [11]. Therefore, as VDR KO and CYP27B1KO represent animal models of severe vitamin D deficiency, they are unsuitable for the detection of the spectrum of tissue sensitivity to early manifestations of vitamin D insensitivity. In an effort to better understand the impact of the loss of one allele of the VDR, we explored the skeletal and metabolic phenotypes of VDR haploinsufficient mice. In this study, we postulated that expression of only one copy of the VDR gene would predispose mice to deleterious changes in body composition and bone mass and make them less responsive to PTH administration. Therefore, initially, we characterized the skeletal phenotype of VDR heterozygous mice by measuring BMD of 8-week-old male and female VDR KO, VDR heterozygous (VDR HET), and wild-type (WT) mice. We also assessed serum PTH levels and in vitro osteoblast differentiation in these animals. The second objective was to longitudinally evaluate the skeletal effects of intermittent PTH administration in VDR heterozygous female mice.

Materials and Methods

The experimental protocols were approved by the Institutional Animal Care and Use Committee of the Maine Medical Center Research Institute. VDR mice used in this study were from a C57/BL6 J background and were purchased from Jackson Laboratory (Bar Harbor, ME). Wildtype (WT or $VDR^{+/+}$), heterozygote (HET or $VDR^{+/-}$), and knockout (KO or $VDR^{-/-}$) were produced from HET × HET breeding. A neomycin resistance gene was inserted in place of exon III of the mouse VDR gene, replacing the second zinc finger of the DNA binding domain. RT-PCR of intestinal and renal RNA from homozygous $VDR^{-/-}$ mice confirmed that a truncated mRNA is expressed from this allele. Heterozygous mice are phenotypically indistinguishable from WT siblings. Homozygous mice exhibit an identical phenotype as the human disease hereditary vitamin D–dependent rickets type 2. Animals were housed in a temperature- and humidity-controlled room and maintained on a 12-h light/12-h dark diurnal cycle. Mice had free access to tap water and standard pellet chow.

Characterization of Bone Phenotype in VDR Heterozygous Mice

Three groups of female and male VDR mice were studied. The male groups were comprised of seven WT, eight HET, and eight KO, whereas the female groups had seven WT, six HET, and nine KO mice. BMD was determined by dual-energy X-ray absorptiometry (DXA) at 8 weeks of age. Bone mass measurement guided the design for further investigation. As total-body and femoral BMD were normal in male mice, we decided to maintain a subgroup of male mice for longitudinal evaluation and to reassess BMD values at 16 weeks to ensure that bone phenotype would be time-dependent. Body composition was also evaluated by DXA in this group. On the other hand, since female mice showed a greater skeletal sensitivity to a possible state of modest vitamin D resistance, the female HET mice were selected for the treatment protocol with PTH administration. Finally, to characterize in vitro osteoblast differentiation and mineralization efficiency, bone marrow cells were flushed from female femurs of the three genotypes (WT, HET, and KO) at 12 weeks of age and subjected to the osteoblast differentiation protocol. Blood samples were collected for determination of serum PTH at 16 weeks of age.

PTH Treatment in WT and VDR Heterozygous Female Mice

Twelve-week-old female mice were divided into four groups: WT + vehicle (VH) ($n = 7$), WT + PTH ($n = 7$), HET + VH ($n = 10$), and HET + PTH ($n = 11$). Mice were subcutaneously (sc) injected with either VH or 50 μg/kg bovine PTH(1–34) (Sigma, St. Louis, MO) 5 days a week for 4 weeks. BMD was determined in basal conditions and at the end of PTH treatment.

Magnetic resonance imaging (MRI) was used to determine whole-body and femur fat content and was performed in three female mice of each group at the end of treatment.

Lumbar spines (L5) and femurs of all female groups were evaluated by micro-computed tomography (μCT). Tibial histomorphometry was performed in five tibial specimens of each mouse group in this experimental protocol.

Bone Marrow Stromal Cell Culture

Tibias and femurs of 12-week-old female WT, HET, and KO were harvested using standardized techniques, as previously described [12]. Briefly, tibias and femurs were collected, and the soft tissues and epiphyses of each bone were removed. The bone marrow was flushed with a 25-gauge needle syringe containing α-MEM supplemented with 10% FBS and 100 U/mL penicillin/streptomycin. A single-cell suspension was obtained by repeated passage through an 18-gauge needle. Cells were plated at 10^7 in a six-well-plate.

On day 7, cells were cultured in differentiation medium containing 8 mM β-glycerophosphate and 50 μg/mL ascorbic acid (Sigma, St. Louis, MO). Cells received fresh medium every other day. After 2 weeks, cell differentiation was assessed using a commercial kit (Diagnostic kit, procedure 86-R; Sigma), to determine colony-forming units (CFUs); and on the same day mineralized nodule formation was determined with alizarin red or von Kossa staining.

BMD and Body Composition Measurements

DXA (Lunar Piximus, software version 1.44.005; Lunar, Madison, WI) was carried out for assessment of femoral BMD, total-body BMD, lean mass, and fat mass. Animals were anesthetized with avertin (2,2,2-tribromoethanol, 250 mg/kg, ip) and placed in a ventral decubitus on an animal tray. The coefficient of variation (CV) for total-body areal BMD was 0.9%.

Femurs were scanned by a μCT instrument (VivaCT-40; Scanco Medical, Basserdorf, Switzerland) to assess cross-sectional geometry at the femoral mid-shaft and trabecular bone volume fraction and microarchitecture in the secondary spongiosa of the distal femur. All scans were analyzed using software (version 4.05, Scanco Medical, Basserdorf, Switzerland) for each area of interest. Femurs were scanned at low resolution, energy level of 55 k Vp and intensity of 145 μA. The VivaCT was calibrated weekly using a phantom provided by Scanco. Scans for the cortical region were measured at the mid-point of each femur, with an isotropic pixel size of 21 μm and slice thickness of 21 μm, and used to calculate the average total cross-sectional area (mm^2), bone area (mm^2), and marrow area (mm^2). For mid-shaft analysis, the cortical shell was contoured by a user-defined threshold and iterated across the 50 slices. Trabecular volume fraction and microarchitecture were evaluated in the secondary spongiosa, starting approximately at 0.6 mm proximal to the growth plate and extending proximally 1.5 mm. We chose 180 consecutive slices from a total of 230 scans of the distal femur, acquired at an isotropic pixel size of 10.5 μm, for analysis. μCT slices for the fifth lumbar vertebral body (L5) were acquired for the entire vertebral body at 10.5 μm. Trabecular bone was evaluated below and above the caudal growth plate regions. In trabecular bone, the CV was 1.8% (total volume [TVμCT]) and 5.5% (bone volume [BVμCT]), whereas in cortical bone the coefficient of variation was 0.15% (TV) and 0.3% (BV).

MRI and ^{1}H Spectroscopy

Axial and coronal images were acquired in a 7.0T Bruker (Billerica, MA) PharmaScan magnet. Animals were anesthetized with inhaled isoflurane 1%, 0.4 L/min. The infused volume was adjusted occasionally, depending on animal respiration frequency. The acquisition method used for body fat was TR 600 ms, TE 87 ms, FOV 40 × 40 × 10 mm, matrix size 256 × 256 × 32, slice thickness 10 mm, one slice, no fat suppression, four average, with a total scan time of about 11 min. For single-pulse spectroscopy, TR 1000 ms, no fat suppression, 400 average, with a total scan time of about 7 min. Femurs were evaluated using the following parameters: 2D RARE8, TR = 2,500 msec, TE = 35.6 msec, matrix = 256 × 256, FOV = 32.5 × 32.5 mm, slice = 0.5 mm, three slices, with fat suppression, five averages, with a total scan time of about 7 min. Spectroscopy was carried out using the following parameters: TR = 2,500 msec, TE = 20 msec, voxel = 0.75 × 7 × 0.75 mm, no fat suppression, 400 average, with a total scan time about 17 min.

Bone Histomorphometry

Mice were intraperitoneally injected with 20 mg/kg calcein and 20 mg/kg demeclocycline on days 9 and 2 before death, respectively. Tibias were removed, dehydrated in ethanol, infiltrated, and embedded without demineralization in methyl methacrylate. Undecalcified

sections were cut at a thickness of 5 μm and mounted unstained for dynamic measurements. Consecutive sections were stained with toluidine blue to quantify bone cells.

Histomorphometric analysis was performed using the OsteoMeasure system (Osteometrics, Decatur, GA), and the results were expressed according to standardized nomenclature [13]. Histomorphometric indexes were as follows: bone volume (BV/TV, %), trabecular thickness (Tb.Th, μm), trabecular number (Tb.N, /mm), trabecular separation (Tb.Sp, μm), mineralizing surface per bone surface (MS/BS, %), mineral apposition rate (MAR, μm/day), bone formation rate per bone surface (BFR/BS, $\mu m^3/\mu m^2$/year), bone formation rate per bone volume (BFR/BV, %/year), bone formation rate per trabecular volume (BFR/TV, %/year), osteoblast surface (Ob.S/BS, %), osteoblast number per trabecular area (N.Ob/T.Ar, /mm^2), osteoblast number per bone perimeter (N.Ob/B.Pm, /mm), osteoid volume (OV/BV, %), osteoid surface (OS/BS, %), osteoid thickness (O.Th, μm), osteoclast surface (Oc.S/BS, %), osteoclast number per trabecular area (N.Oc/T.Ar, /mm^2) osteoclast number per bone perimeter (N.Oc/B.Pm, /mm), and eroded surface (ES/BS, %).

Biochemical Analyses

Intact PTH was measured in serum by two-site enzyme-linked immunosorbent assay (Immutopics, San Clement, CA). Intra- and interassay variations were 3.2% and 8.4%, respectively.

Statistical Analysis

We used ANOVA, through a GLM procedure of SAS 9.0 software (SAS Institute, Cary, NC), to compare the following groups: (1) BMD and body composition assessed by DXA (Piximus) in male (WT, VDR HET, VDR KO) mice at the age of 8 weeks; (2) BMD, fat mass, and lean mass gain in male (WT, VDR HET, and VDR KO) and female (WT, VDR HET, and VDR KO) mice aged 8–16 weeks; (3) serum levels of PTH in male (WT, VDR HET, VDR KO) and female (WT, VDR HET, VDR KO) mice; (4) BMD gain in female mice treated with vehicle or PTH (WT VH, WT PTH, VDR HET VH, VDR HET PTH); (5) bone histomorphometric parameters obtained in female mice after vehicle or PTH therapy; and (6) bone parameters of μCT measured in female mice after vehicle or PTH therapy. As we had a dependence between data of groups and time, comparisons were made through a mixed model, using the MIXED procedure of SAS 9.0 software in the following analysis: (1) BMD and body composition assessment in WT, VDR HET, and VDR KO female and male mice aged 8 and 16 weeks and (2) ecocardiographic assessment before and after 4 weeks of vehicle or PTH therapy in female mice (WT VH, WT PTH, VDR HET VH, VDR HET PTH). To compare the data of μCT parameters in female groups (WT and HET) at age 16 weeks, Student's *t*-test was applied using the PROC T TEST of SAS 9.0.

Results

Skeletal Phenotypes in VDR Male and Female HET Mice

Male Mice—Not unexpectedly, on a regular chow diet, 8-week-old VDR KO males had significantly lower total-body and femur BMD than VDR HET and WT mice (Fig. 1a). However, BMD values at both sites in VDR HET males were similar to those in WT males. The same BMD pattern was observed in the three genotypes at 16 weeks of age. Hence, there were no significant differences in the rate of bone acquisition among males with VDR KO, VDR HET, and WT genotypes (Fig. 1b). Regarding other body composition parameters, there were no significant differences in lean mass among the three male genotypes. However, WT male mice showed a greater increase in lean mass than VDR KO (3.76 ± 1.47 vs. 1.39 ± 1.32 g, $P < 0.05$) and VDR HET (3.39 ± 1.05 vs. 1.39 ± 1.32 g, $P < 0.05$) mice during the observation period. There was no significant difference in lean mass

gain between WT and HET male mice. Fat mass content, at 8 weeks, was less in VDR KO (2.22 ± 0.38 g) male mice than in HET (3.31 ± 0.69, $P < 0.05$) and WT (3.33 ± 0.69 g) male mice. Furthermore, fat mass gain was significantly less in VDR HET (+1.48 ± 0.65, $P < 0.05$) and VDR KO (+0.57 ± 0.38 g; $P < 0.05$) male mice than in WT males (+3.14 ± 1.51 g). Fat mass gain was significantly higher in VDR HET male mice in comparison to VDR KO male mice, $P < 0.05$ (Fig. 1c).

Female Mice—Total-body BMD was significantly greater in WT female mice (0.0465 ± 0.001 g/cm^2) than in VDR HET (0.0431 ± 0.003 g/cm^2, $P < 0.05$) and VDR KO (0.0289 ± 0.002 g/cm^2 $P < 0.05$) female mice. Also, there was a significant difference in total-body BMD between VDR HET and KO mice ($P < 0.05$, Fig. 2). In the femur, BMD in female VDR HET (0.04858 ± 0.0027 g/cm^2) mice was slightly, but not significantly, decreased in comparison to WT female mice at 8 weeks (0.05119 ± 0.0023 g/cm^2) (Fig. 2). However, femoral BMD of VDR KO female mice (0.03146 ± 0.0036 g/cm^2) was significantly lower than that of female VDR HET ($P < 0.05$) and WT ($P < 0.05$) mice at 8 weeks of age. On the other hand, fat mass was slightly decreased in VDR KO female mice at 8 weeks of age, but body fat content was similar between VDR HET and WT female mice in this period. There was no significant difference in the lean mass of these three groups during the same interval.

At 16 weeks of age, the skeletal microarchitecture of L5 and the femur was evaluated in VDR HET and WT female groups by μCT. In L5, bone volume (BV) was significantly decreased in VDR HET (0.33 ± 0.050) in comparison to WT female mice (0.40 ± 0.03), $P < 0.05$. In addition, there was a trend among VDR HET mice to exhibit lower BV/TV (23.93 ± 1.57% vs. 29.40 ± 4.82%, $P < 0.06$) and higher trabecular separation (0.24 ± 0.020 vs. 0.21 ± 0.030, $P < 0.06$) than WT mice (Fig. 3a). In concordance with the DXA evaluation, μCT assessment in the femur did not show a significant difference between female HET and WT mice. Figure 3b shows the cortical phenotype of femurs from both groups.

As expected, VDR KO mice had a significantly higher serum PTH level than VDR HET and WT ($P < 0.05$). However, serum PTH levels were only slightly and not statistically higher in VDR HET compared to WT mice. There was a trend for higher PTH levels in both female and male VDR HETs, but this did not reach statistical significance and was very modest compared to the very high levels of PTH in VDR KO mice (WT = 49.4 ± 20.7 vs. HET = 67.57 ± 45.70 vs. KO = 2,739 ± 1,575 pg/mL) and females (WT = 69 ± 42.88 vs. HET = 83.84 ± 36.26 vs. KO = 4,390 ± 3,206 pg/mL). It was also observed that male mice in the three groups had nonsignificantly lower PTH levels than female mice.

To determine whether the reduced bone mass in the VDR HET group was related to a cell autonomous effect due to the absence of one allele of the VDR gene, we performed in vitro differentiation studies. As expected, there was a significant impairment in bone marrow stromal cell (BMSC) differentiation capacity in VDR KO mice at age 12 weeks, observed during the preosteoblast phase and with osteoblast differentiation and mineralization (Fig. 4a). This was reflected on day 14 of BMSC cultures, when the number of cells was strikingly reduced in KO relative to WT cells. Similarly, the mineralization process, as measured by von Kossa (Fig. 4a) and alizarin red (Fig. 4b) staining, was also decreased in the KO mouse cells. Interestingly, both alkaline phosphatase and von Kossa staining of cells from the VDR HET group revealed an intermediate phenotype between VDR KO and WT (Fig. 4a).

Bone Mass and Body Composition in VDR Female HET Mice: Response to PTH Treatment

Based on a modest skeletal phenotype in the VDR HETs, we hypothesized that absence of one allele in the VDR gene might impair the skeletal anabolic response to PTH. Therefore, female VDR HET and WT mice were treated with PTH 5 days a week for 4 weeks. Figure

5a and b shows total-body and femur BMD values in WT and VDR HET female mice at 12 weeks of age in basal conditions and after 4 weeks of intermittent PTH or (VH) treatment. WT female mice treated with VH exhibited significantly higher BMD for total body (Fig. 5a) and femur (Fig. 5b) at the end of treatment, while the femoral BMD value in VDR HET female mice, which received VH, at age 16 weeks was similar to that obtained at 12 weeks. Total-body and femur BMD in WT and VDR HET female mice treated with PTH at the age of 16 weeks were significantly higher than before treatment (e.g., BMD in total body before and after PTH treatment, WT: 12 weeks = 0.0513 ± 0.0018 vs. 16 weeks = 0.0543 ± 0.0021, HET: 12 weeks = 0.0507 ± 0.002495 vs. 16 weeks = 0.0542 ± 0.0022, g/cm^2; $P < 0.05$). Absolute total-body BMD gain in 4 weeks after PTH treatment corresponded to 0.0021 ± 0.0012 g/cm^2 in WT VH, 0.0031 ± 0.0016 g/cm^2 in WT PTH, 0.0018 ± 0.0010 g/cm^2 in HET VH, and 0.0035 ± 0.0011 g/cm^2 in HET PTH. μCT of L5, in the four groups, revealed a similar pattern of bone structure as observed in the femur (Table 1).

Changes in femoral BMD in these mice are shown in Fig. 5b. There was no significant difference in femoral BMD between HET and WT female mice treated with vehicle. However, WT mice receiving vehicle had significantly enhanced BMD during the 4-week period (T1: WT VH = 0.0560 ± 0.0029 vs. T2: WT VH = 0.0597 ± 0.00296, g/cm^2; $P < 0.05$), while HET females maintained stable femoral BMD (T1: HET VH = 0.0595 ± 0.0046 vs. T2: HET VH = 0.06021 ± 0.0034, g/cm^2). Both WT and HET females showed significant enhancement in BMD after PTH treatment (WT: T1 = 0.0585 ± 0.0018 vs. T2 = 0.0657 ± 0.00164, $P < 0.01$; HET: T1 = 0.0564 ± 0.0038 vs. 16 weeks = 0.0634 ± 0.0032, g/cm^2). Bone mass gain corresponded to 0.0042 ± 0.0012 g/cm^2 in WT female mice after VH, 0.0071 ± 0.0022 g/cm^2 in WT female mice after PTH, 0.0008 ± 0.0020 g/cm^2 in HET female mice injected with VH and 0.0070 ± 0.0024 g/cm^2 in HET female mice injected with PTH. Femoral bone mass gain in WT female mice receiving vehicle was not significantly different from that in WT female mice after sc PTH injection. The enhancement of femoral BMD was of the same magnitude in VDR HET and WT undergoing PTH treatment.

In agreement with the results obtained by BMD and μCT, histomorphometric analysis showed that deletion of a single allele of the VDR gene was associated with a mild skeletal phenotype. Bone volume in VDR HET female mice was not different from that in WT female mice. However, mineralizing surface and bone formation rate per tissue volume were decreased in VDR HET compared to WT. There were subtle differences in bone dynamic parameters after PTH treatment between HET and WT female mice. PTH treatment in HET female mice was associated with significant increment in bone formation rate (BFR/BS, BFR/BV, and BFR/TV) in comparison to the corresponding VH-treated mice. WT mice treated with PTH exhibited a nonsignificant increase in BFR/BS and BFR/BV, but BFR/TV was higher in comparison to WT mice treated with VH (Table 2). On the other hand, VDR HET and WT female mice showed a significant response to PTH treatment in comparison to the corresponding genotype receiving VH in relation to the following parameters ObS/BS, N.Ob/T.Ar, and N.Ob/B.Pm (Table 2).

Bone structure was further studied by μCT in femur and L5. Table 2 shows these results. Femoral bone mass in VDR HET mice was similar to that in WT mice (BV/TV: WT VH = 3.40 ± 1.7% vs. HET VH = 3.50 ± 1.2%). There was a nonsignificant difference in femoral connectivity density by μCT after PTH treatment. However, the group of female HET treated with PTH had a significantly higher trabecular thickness (HET VH = 36.60 ± 3.70 vs. HET PTH = 41.30 ± 4.50 μm, $P < 0.05$) than female HET injected with VH with a trend in BV/TV (HET VH = 3.50 ± 1.2% vs. HET PTH = 4.7 ± 1.5 %). Meanwhile, WT female mice had significant changes in bone mass after PTH therapy. Cortical thickness values were similar in the four groups. There was no significant difference in BV/TV and connectivity density measured by μCT among the groups in L5. However, trabecular

thickness was significantly higher in HET mice treated with PTH than HET mice treated with vehicle. PTH therapy did not change significantly the trabecular thickness in WT mice. Figure 6 shows the microstructure of L5 and the femur (trabecular and cortical bone) in WT and VDR HET mice treated with vehicle or PTH.

Lean mass content was very similar in the four groups during the period of evaluation. Although VDR HET female mice had a tendency to gain more lean mass than WT female mice, there was no significant difference between the groups. The opposite trend was observed in relation to fat mass gain between the groups; female HET mice gained less fat mass than WT, but the differences were not statistically significant. It was observed that while VDR HET female mice, especially those on VH treatment, had a decrease in percent fat, the WT showed an increase in this parameter (WT VH = +1.63%, WT PTH = +2.7%, HET VH = −0.52%, and HET PTH = +0.58%). Figure 7 shows body fat measured by MRI. There were no differences in fat mass content between groups, but both genotypes treated with PTH showed a tendency to gain fat mass.

Discussion

In this study we suggest that heterozygosity in the VDR gene is associated with a mild skeletal and anthropomorphic phenotype that is gender-specific. We initiated this work because of the growing body of evidence that circulating levels of serum 25(OH)D have been associated with chronic disorders including osteoporosis, diabetes mellitus, and atherosclerosis as well as altered metabolic homeostasis [8, 14–17]. However, experimental animal models with modestly low vitamin D are not common and often not illustrative. On the other hand, severe vitamin D deficiency and resistant states can be studied in the Cyp27B1 and VDR KO mouse models, which are analogous to rare cases of severe vitamin D deficiency known as vitamin D–dependent rickets types 1 and type 2, respectively, in humans.

Using the VDR HET mouse as a model, we hypothesized that the absence of one allele in the VDR would have a significant impact on body composition, lean mass, and the skeletal response to PTH. Indeed, we found that VDR heterozygotic mice showed differences, albeit small, in bone mass and body composition that were gender- and age-specific. In particular, VDR HETs had a modest but nonsignificant increase in serum PTH and reduced total-body areal BMD and vertebral BV/TV in females compared to WT controls. Yet, VDR HET female mice showed a normal skeletal response to PTH treatment without vitamin D and/or calcium supplementation. Interestingly, male VDR HETs exhibited less gain in fat mass with age than WT but more than male VDR KO mice.

We acknowledge that this study has some limitations, especially because the number of animals studied in each group was small. In contrast, we have characterized bone structure in female HET mice by three different methods. Body composition in male mice was examined prospectively, and the results are consistent with previous studies showing that lean phenotype is a trait of male VDR KO mice which is accentuated by age [18]. Surprisingly, few studies have evaluated gender-related influences on the clinical manifestations of vitamin D deficiency. A recent study verified that mortality was more pronounced among women than men harboring vitamin D deficiency [19]. The present study shows that the impairment in bone acquisition is an early event in female VDR HET mice. Differences in BMD were observed as early as 8 weeks of age. On the other hand, male VDR HET mice exhibited increases in BMD similar to WT mice between 8 and 16 weeks of age. Previously [20], decreased fertility was observed in VDR HET mice, but neither female VDR HET nor male VDR HET mice had abnormal estradiol or testosterone serum levels, respectively, although they exhibited decreased fertility. However, another study showed

that estrogen has tissue-specific effects on the regulation of VDR expression [21]. And it was observed in castrated males and oophorectomized female rats that estradiol administration upregulated VDR expression in liver, downregulated VDR in kidney, and had neutral effects on the intestine. On the other hand, testosterone had no effect on VDR regulation in gonadectomized rat. These observations support potential gender differences in the vitamin D–deficient state.

The vitamin D–PTH axis was not significantly affected in female VDR HET mice at age 16 weeks since PTH serum levels were nearly the same in male and female VDR HETs and not different from those in WT. Our results are in accordance with those obtained previously by Erben et al. [22], who verified a late impact in the skeleton of male mice with a single-allele mutation in the VDR gene. These authors also showed that VDR HET mice have PTH elevations at age 6 months. Furthermore, there are studies showing that a strong correlation between vitamin D deficiency and secondary hyperparathyroidism emerges in circumstances of severe vitamin D deficiency [23, 24].

In addition to the in vivo parameters of the bone phenotype in female VDR HET mice, BMSC differentiation into osteoblasts was found to be blunted in the heterozygotes. In a previous study, it was demonstrated, by 4 months of age, that VDR null mice have a reduction in CFU-OBs, accompanied by a decrease in trabecular bone volume [25]. This was confirmed in our studies, and as mentioned, there were intermediate changes in marrow cells from VDR HET. However, in vitro studies of the HETs were much more pronounced than the in vivo skeletal phenotypes, suggesting the possibility of compensation at the whole-body level or differences in culture techniques.

Clinical investigations have often shown that obese individuals have low 25(OH)D serum levels [26, 27]. Also, some [28, 29], but not all [30], studies have shown that circulatory 25(OH)D increases after bariatric surgery, suggesting that after adipose tissue shrinkage previously accumulated vitamin D is released into the extracellular fluid. Surprisingly, recent studies have shown that VDR KO [18, 31] and CYP27B1KO [31] mice have a lean phenotype and a trend toward improved glucose tolerance and insulin sensitivity [31]. In the present study, differences in body weight between VDR HET mice and their WT counterparts were not observed. However, male VDR HET mice had less fat mass gain during the study interval than WT males. This was not observed in female mice, corresponding to another gender-related difference in VDR HET mice. The more pronounced lean phenotype in male than female VDR KO mice was observed in a previous study [18]. Our data contribute to this line of investigation, showing that adipose tissue in male mice is exquisitely sensitive to changes in VDR action. However, there is an apparent contradiction between results showing a clinical association of obesity to vitamin D deficiency and VDR KO and Cyp27B1 mice, which are lean [3]. Actually, concomitant with the low serum levels of 25(OH)D, obese patients usually have higher $1,25(OH)_2D$ levels [32]. $1,25(OH)_2D$ promotes lipogenesis and inhibits lipolysis through stimulation of ionized calcium (Ca^{2+}) with the expression and activity of fatty acid synthase, a step-limiting enzyme in lipogenesis [33, 34]. The influx of Ca^{2+} into adipocytes corresponds to an alternative nongenomic action of vitamin D, most likely resulting from its interaction with a putative membrane receptor [35]. Notwith-standing, our study does not address the mechanism responsible for the inverse association between endogenous 25(OH)D levels and obesity. Further studies of the VDR HET on a high-fat diet are planned.

Conclusions

In summary, the present study indicates that the VDR HET mouse has a mild skeletal and metabolic phenotype. These mice may be a useful experimental model for investigating the

effects of vitamin D resistance on skeletal and adipose tissue. Additionally, our results suggest that gender and possibly age exert influences on the phenotypic presentation of VDR heterozygous mice.

Acknowledgments

We thank Terry M. Handerson and Marilena Preda for technical assistance in μCT and MRI exams, respectively. F. J. A. P. received financial support from the National Council for Scientific and Technological Development (CNPq), Brazil (201650/2008-8). I. D.-P. received financial support from CAPES, Brazil (0102-09-1).

References

1. DeLuca HF. Overview of general physiologic features and functions of vitamin D. Am J Clin Nutr. 2004; 80:1689S–1696S. [PubMed: 15585789]
2. Holick MF. Ressurrection of vitamin D deficiency and rickets. J Clin Invest. 2006; 116:2062–2072. [PubMed: 16886050]
3. Adams JS, Hewison M. Update in vitamin D. J Clin Endocrinol Metab. 2010; 95:471–478. [PubMed: 20133466]
4. Kuchuk NO, van Schoor NM, Pluijm SM, Chines A, Lips P. Vitamin D status, parathyroid function, bone turnover and BMD in postmenopausal women with osteoporosis: global perspective. J Bone Miner Res. 2009; 24:693–701. [PubMed: 19049341]
5. Elsammak MY, Al-Wosaibi AA, Al-Howeish A, Alsaeed J. Vitamin D deficiency in Saudi Arabs. Horm Metab Res. 2010; 42:364–368. [PubMed: 20213587]
6. Amling M, Priemel M, Holzmann T, Chapin K, Rueger JM, Baron R, Demay MB. Rescue of the skeletal phenotype of vitamin D receptor–ablated mice in the setting of normal mineral ion homeostasis: formal histomorphometric and biomechanical analyses. Endocrinology. 1999; 140:4982–4987. [PubMed: 10537122]
7. Zheng W, Xie Y, Li G, Kong J, Feng JQ, Li YC. Critical role of calbindin-D28 k in calcium homeostasis revealed by mice lacking both vitamin D receptor and calbindin-D28 k. J Biol Chem. 2004; 279:52406–52413. [PubMed: 15456794]
8. Bouillon R, Carmeliet G, Verlinden L, van Etten E, Verstuyf A, Luderer HF, Lieben L, Mathieu C, Demay M. Vitamin D and human health: lessons from vitamin D receptor null mice. Endocr Rev. 2008; 29:726–776. [PubMed: 18694980]
9. Verstuyf A, Carmeliet G, Bouillon R, Mathieu C. Vitamin D: a pleiotropic hormone. Kidney Int. 2010; 78:140–145. [PubMed: 20182414]
10. Gallagher JC, Sai AJ. Vitamin D insufficiency, deficiency and bone health. J Clin Endocrinol Metab. 2010; 95:2630–2633. [PubMed: 20525913]
11. Stechschulte SA, Kirsner RS, Federman DG. Vitamin D: bone and beyond, rationale and recommendations for supplementation. Am J Med. 2009; 122:793–802. [PubMed: 19699370]
12. Lecka-Czernick B, Ackert-Bicknell C, Adamo L, Marmolejos V, Churchill GA, Shockley KR, Reid IR, Grey A, Rosen CJ. Activation of peroxisome proliferator-activated receptor gamma (PPARgamma) by rosiglitazone suppresses components of the insulin-like growth factor regulatory system in vitro and in vivo. Endocrinology. 2007; 148:903–911. [PubMed: 17122083]
13. Parfitt AM, Drezner MK, Glorieux FH, Kanis JA, Malluche H, Meunier PJ, Ott SM, Recker RR. Bone histomorphometry: standardization of nomenclature, symbols and units. Report of the ASBMR Histomorphometry Nomenclature Committee. J Bone Miner Res. 1987; 2:595–610. [PubMed: 3455637]
14. Bischoff-Ferrari HA, Dawson-Hughes B, Staehelin HB, Orav JE, Stuck AE, Theiler R, Wong JB, Egli A, Kiel DP, Henschkowski J. Fall prevention with supplemental and active forms of vitamin D: a meta-analysis of randomised controlled trials. BMJ. 2009; 339:b3692. [PubMed: 19797342]
15. Panda DK, Miao D, Tremblay ML, Sirois J, Farookhi R, Hendy GN, Goltzman D. Targeted ablation of the 25-hydroxyvitamin D 1α-hydroxylase enzyme: evidence for skeletal, reproductive and immune dysfunction. Proc Natl Acad Sci USA. 2001; 98:7498–7503. [PubMed: 11416220]

16. Dardenenne O, Prud'homme J, Hacking SA, Glorieux FH, St. Arnaud R. Rescue of the pseudo-vitamin D deficiency rickets phenotype of CYP27B1-deficient mice by treatment with 1,25-dihydroxyvitamin D3: biochemical, histomorphometric, and biomechanical analyses. J Bone Miner Res. 2003; 18:637–643. [PubMed: 12674324]

17. Adams JS, Hewison M. Unexpected actions of vitamin D: new perspectives on the regulation of innate and adaptive immunity. Nat Clin Pract Endocrinol Metab. 2008; 4:80–90. [PubMed: 18212810]

18. Wong KE, Szeto FL, Zhang W, Honggang Y, Kong J, Zhang Z, Sun XJ, Li YC. Involvement of the vitamin D receptor in energy metabolism regulation of uncoupling proteins. Am J Physiol Endocrinol Metab. 2009; 296:E820–E828. [PubMed: 19176352]

19. Melamed ML, Michos ED, Post W, Astor B. 25-Hydroxyvitamin D levels and the risk of mortality in the general population. Arch Intern Med. 2008; 168:1629–1637. [PubMed: 18695076]

20. Kinuta K, Tanaka H, Moriwake T, Aya K, Kato S, Seino Y. Vitamin D is an important factor in estrogen biosynthesis of both female and male gonads. Endocrinology. 2000; 141:1317–1324. [PubMed: 10746634]

21. Duncan WE, Glass AR, Wray HL. Estrogen regulation of the nuclear 1,25-dihydroxyvitamin D3 receptor in rat liver and kidney. Endocrinology. 1991; 129:2318–2324. [PubMed: 1657571]

22. Erben RG, Soegiarto DW, Weber K, Zeitz U, Lieberherr M, Gniadecki R, Möller G, Adamski J, Balling R. Deletion of deoxyribonucleic acid binding domain of the vitamin D receptor abrogates genomic and nongenomic functions of vitamin D. Mol Endocrinol. 2002; 16:1524–1537. [PubMed: 12089348]

23. Binkley N, Novotny R, Krueger D, Kawahara T, Daida YG, Lensmeyer G, Hollis BW, Drezner MK. Low vitamin D status despite abundant sun exposure. J Clin Endocrinol Metab. 2007; 92:2130–2135. [PubMed: 17426097]

24. Lips P. Vitamin D deficiency and secondary hyperpara-thyroidism in the elderly: consequences for bone loss and fractures and therapeutic implications. Endocr Rev. 2001; 22:477–501. [PubMed: 11493580]

25. Panda DK, Miao D, Bolivar I, Li J, Huo R, Hendy GN, Goltzman D. Inactivation of the 25-hydroxyvitamin D 1alpha-hydroxylase and vitamin D receptor demonstrates independent and interdependent effects of calcium and vitamin D on skeletal and mineral homeostasis. J Biol Chem. 2004; 279:16754–16766. [PubMed: 14739296]

26. Liel Y, Ulmer E, Shary J, Hollis BW, Bell NH. Low circulating vitamin D in obesity. Calcif Tissue Int. 1988; 43:199–201. [PubMed: 3145124]

27. Snijder MB, van Dam RM, Visser M, Deeg DJ, Dekker JM, Bouter LM, Seidell JC, Lips P. Adiposity in relation to vitamin D status and parathyroid hormone levels: a population-based study in older men and women. J Clin Endocrinol Metab. 2005; 90:4119–4123. [PubMed: 15855256]

28. de Luis DA, Pacheco D, Izaola O, Terroba MC, Cuellar L, Martin T. Clinical results and nutritional consequences of bilio-pancreatic diversion: three years of follow up. Am Nutr Metab. 2008; 53:234–239.

29. Pereira FA, Castro JAS, Santos JE, Foss MC, Paula FJ. Impact of marked weight loss induced by bariatric surgery on bone mineral density and remodeling. Braz J Med Biol Res. 2007; 40:509–517. [PubMed: 17401494]

30. Jin J, Robinson AV, Hallowell PT, Jasper JJ, Stellato TA, Wilhem SM. Increases in parathyroid hormone after gastric bypass appear to be of secondary nature. Surgery. 2007; 142:914–920. [PubMed: 18063076]

31. Narvaez CJ, Matthews D, Broun E, Chan M, Welsh J. Lean phenotype and resistance to diet-induced obesity in vitamin D receptor knockout mice correlates with induction of uncoupling protein-1 in white adipose tissue. Endocrinology. 2009; 150:651–661. [PubMed: 18845643]

32. Hey H, Stokholm KH, Lund B, Lund B, Sørensen OH. Vitamin D deficiency in obese patients and changes in circulating vitamin D metabolites following jejunoileal bypass. Int J Obes. 1982; 6:473–479. [PubMed: 6983505]

33. Zemel MB, Kim JH, Woychik RP, Michaud EJ, Kadwell SH, Patel IR, Wilkison WO. Agouti regulation of intracellular calcium: role in the insulin resistance of viable yellow mice. Proc Natl Acad Sci USA. 1995; 92:4733–4737. [PubMed: 7761392]

34. Shi H, Norman AW, Okamura WH, Sen A, Zemel MB. 1*α*,25-Dihydroxyvitamin D3 inhibits uncoupling protein 2 expression in human adipocytes. J FASEB. 2002; 16:1808–1810.

35. Holmén J, Jansson A, Larsson DA. kinetic overview of the receptors involved in 1,25-dihydroxyvitamin D3 and 24,25-dihydroxyvitamin D3 signaling: a systems biology approach. Crit Rev Eukaryot Gene Expr. 2009; 19:181–196. [PubMed: 19883364]

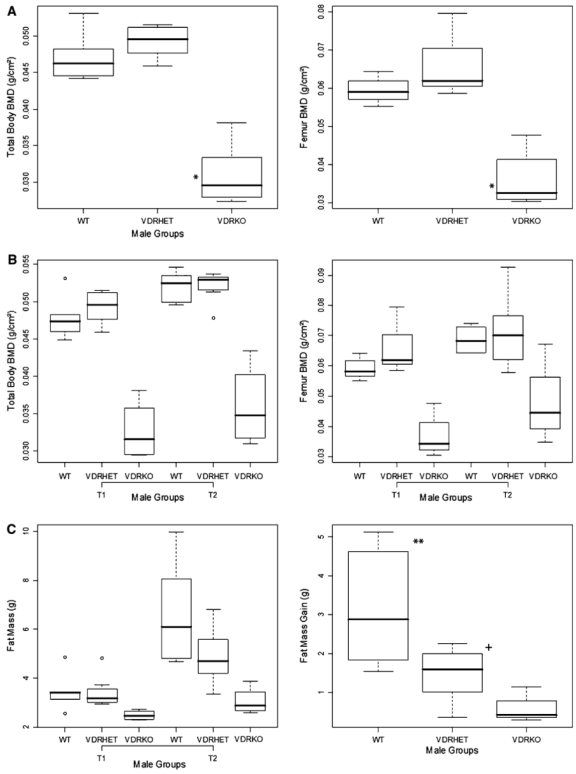

Fig. 1.

a Total-body (*left*) and femur BMD (*right*) in VDR WT, HET, and KO male mice at 8 weeks of age. **b** Total-body (*left*) and femur BMD (*right*) in VDR WT, HET, and KO male mice at 8 and 16 weeks of age. **c** Total-body fat mass content (*left*) and fat mass gain (*right*) during an 8-week interval in VDR WT, HET, and KO mice. *Values significantly smaller in KO than in HET and WT mice, $P < 0.05$; **values significantly greater in WT than in HET and KO mice, $P < 0.05$; $^{+}$values significantly smaller in KO than in HET mice

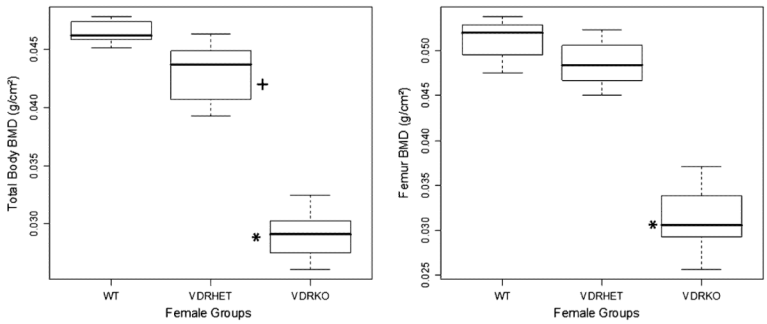

Fig. 2.

Total-body (*left*) and femur (*right*) BMD in 8-week-old VDR WT, HET, and KO female mice. *Values significantly smaller in KO mice than in WT and HET mice; $^{+}$values higher in WT than in HET mice, $P < 0.05$

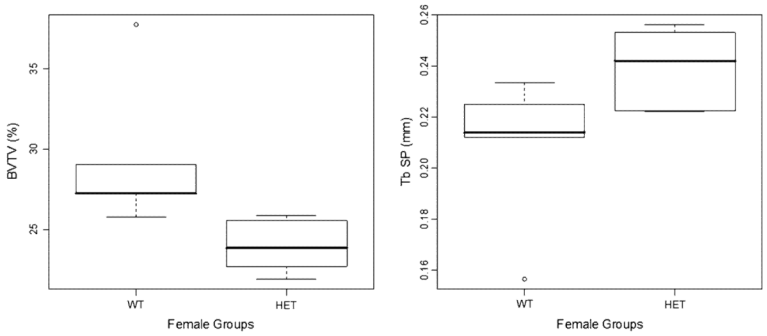

Fig. 3.

μCT analysis showing bone volume (BV/TV) (*left*) and trabecular separation (*right*) in VDR WT and HET mice at 16 weeks of age

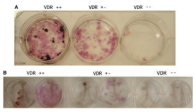

Fig. 4.

Effect of a single-allele mutation on osteoblast differentiation. The number of ALP^+ colonies at day 14 is decreased in VDR HET female mice, and further impairment is verified in VDR KO mice. Subsequent evaluation of mineralization activity by von Kossa (**a**) and alizarin red (**b**) shows the same defect pattern in the tree genotype

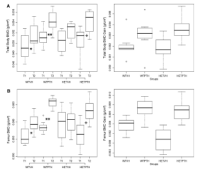

Fig. 5.

a BMD in total body (*left*) and total-body bone mass gain (*right*) in VDR WT and HET female mice at age 12 weeks and after 4 weeks of treatment with vehicle (VH) or parathyroid hormone (PTH). **b** BMD in femur (*left*) and femoral bone mass gain (*right*) in VDR WT and HET female mice at age 12 weeks and after 4 weeks of treatment with VH or PTH. *Basal BMD (12 weeks, T1) values in WT female mice smaller than after VH treatment (16 weeks); **basal BMD (12 weeks, T1) values in WT female mice smaller than after PTH treatment; $^{+}$basal BMD (12 weeks, T1) values in HET female mice smaller than after PTH treatment, $P < 0.05$

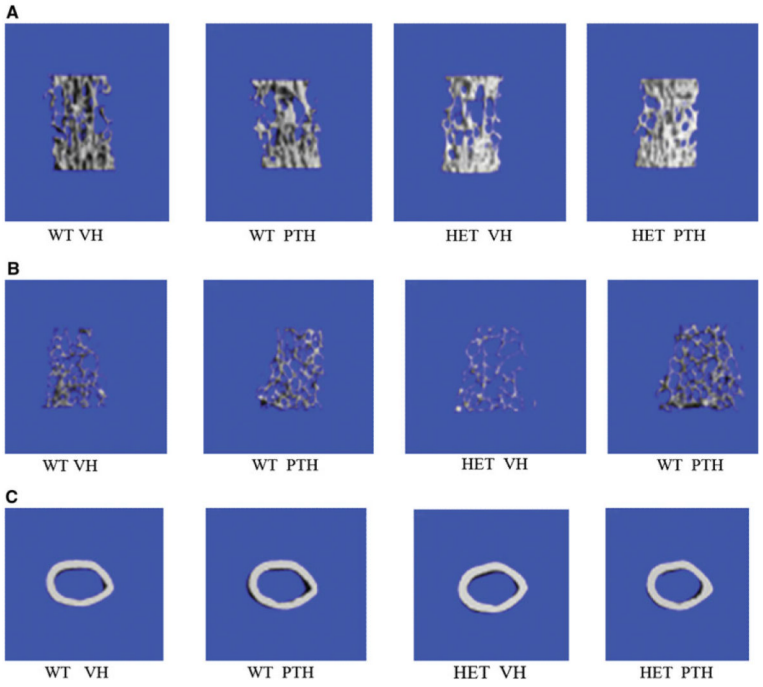

Fig. 6.

μCT images of lumbar vertebra cancellous bone (L5) (**a**), distal femur cancellous bone (**b**), and femur cortical bone (**c**) in WT female mice treated with vehicle (WT VH) or PTH (WT PTH) and heterozygous female mice treated with vehicle (HET VH) or PTH (HET PTH)

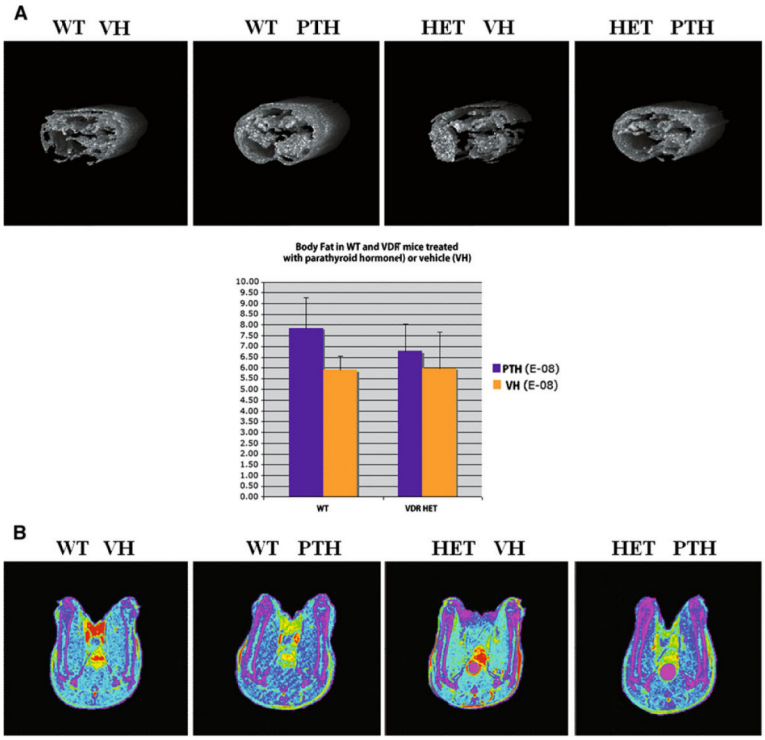

Fig. 7.

Body fat content (**a**) and femoral fat content (**b**) assessed by MRI in WT female mice treated with vehicle (WT VH) or PTH (WT PTH) and heterozygous female mice treated with vehicle (HET VH) and PTH (HET PTH)

Table 1

Bone structural parameters measured by μCT in WT and VDR HET female mice treated with vehicle (VH) or PTH for 4 weeks

	WT VH (*n* = 7)	WT PTH (*n* = 7)	HET VH (*n* = 9)	HET PTH (*n* = 9)
L5				
Cancellous BV/TV (%)	26.13 ± 4.08	31.03 ± 3.15	28.10 ± 3.43	29.92 ± 2.51
Tb.Th (μm)	57.13 ± 4.74*	61.37 ± 1.84	57.31 ± 1.84*	61.10 ± 1.82
Tb.N (1/mm)	4.43 ± 0.32	4.82 ± 0.36	4.77 ± 0.67	4.54 ± 0.42
Tb.Sp (μm)	271 ± 20.1	207 ± 24.2	209 ± 33.8	219 ± 22.8
Conn.D (1/mm^3)	134 ± 14.9	163.9 ± 26.3	156 ± 28.5	158.8 ± 22.2
Femur				
Cancellous BV/TV (%)	3.4 ± 1.70*	5.45 ± 0.83	3.50 ± 1.20	4.7 ± 1.50
Tb.Th (μm)	35.9 ± 5.70*	42.50 ± 3.13	36.60 ± 3.7*	41.30 ± 4.5
Tb.N (1/mm)	2.75 ± 0.46	2.86 ± 0.37	2.91 ± 0.31	2.77 ± 0.45
Tb.Sp (μm)	370 ± 71.9	350 ± 55.3	347 ± 39.5	367 ± 77.2
Conn.D (1/mm^3)	35.9 ± 21.8	54.7 ± 15.8	31.5 ± 19.3	46.6 ± 20.2
Cortical Th. (μm)	217 ± 7.7	224 ± 7.7	218 ± 7.7	224 ± 10.1

* Significant difference between VH and PTH treatment in the same genotype (P<0.05)

Table 2

Histomorphometric parameters in WT and VDR HET female mice treated with vehicle (VH) or PTH for 4 weeks

Parameters	WT VH (*n* = 5)	WT PTH (*n* = 5)	HET VH (*n* = 6)	HET PTH (*n* = 6)	ANOVA *P*
BV/TV (%)	3.72 ± 1.19	4.62 ± 0.48	2.15 ± 0.32	3.54 ± 0.96	0.15
Tb.Th (μm)	32.52 ± 4.24	36.03 ± 2.35	26.41 ± 2.26	34.86 ± 4.68	0.17
Tb.N (/mm)	1.06 ± 0.18	1.28 ± 0.10	0.80 ± 0.08	0.96 ± 0.20	0.19
Tb.Sp (μm)	993 ± 128	769 ± 72	1,298 ± 162	1,314 ± 318	0.19
MS/BS (%)	30.19 ± 3.12	29.42 ± 2.06	19.21 ± 2.59	28.35 ± 4.50	0.07
MAR (μm/day)	1.90 ± 0.31	2.83 ± 0.29*	2.06 ± 0.14	2.52 ± 0.22	0.04
BFR/BS ($\mu m^3/\mu m^2$/year)	201 ± 26	295 ± 6	141 ± 17	273 ± 61*	0.01
BFR/BV (%/year)	1,293 ± 210	1,726 ± 107	986 ± 123	1,486 ± 245*	0.03
BFR/TV (%/year)	43 ±9	71 ± 6*	23 ±3	53 ± 13*	0.02
Ob.S/BS (%)	4.41 ± 1.73	12.53 ± 1.69*	6.85 ± 2.74	14.06 ± 3.13*	0.01
N.Ob/T.Ar (/mm^2)	8.60 ± 4.70	27.08 ± 4.06*	9.81 ± 4.37	19.20 ± 3.19*	<0.01
N.Ob/B.Pm (/mm)	3.35 ± 1.21	10.78 ± 1.56*	5.95 ± 2.31	11.46 ± 2.25*	<0.01
OV/TV (%)	0.017 ± 0.012	0.038 ± 0.007	0.018 ± 0.015	0.033 ± 0.009	0.31
OS/BS (%)	2.26 ± 0.98	5.46 ± 1.38	4.96 ± 3.54	7.99 ± 2.38	0.24
O.Th (μm)	1.95 ± 0.54	3.19 ± 0.75	0.95 ± 0.44	2.73 ± 0.25	0.26
Oc.S/BS (%)	2.14 ± 0.59	1.21 ± 0.63	1.87 ± 0.58	3.51 ± 1.05	0.23
N.Oc/T.Ar (/mm^2)	1.82 ± 0.43	1.79 ± 0.96	1.49 ± 0.52	2.68 ± 0.82	0.66
N.Oc/B.Pm (/mm)	0.88 ± 0.23	0.63 ± 0.32	0.89 ± 0.26	1.33 ± 0.30	0.36
ES/BS (%)	1.72 ± 0.49	0.79 ± 0.30	0.67 ± 0.38	2.48 ± 1.11	0.64

*Significant difference between VH and PTH treatment in the same genotype ($P<0.05$)